

# Supramolecular Hybrid Material Constructed from Graphene Oxide and Pillar[6]arene-Based Host–Guest Complex as a Ultrasound and Photoacoustic Signals Nanoamplifier

Guocan Yu,<sup>a#</sup> Jie Yang,<sup>b#</sup> Xiao Fu,<sup>a#</sup> Zhantong Wang,<sup>a</sup> Li Shao,<sup>b</sup> Zhengwei Mao,<sup>\*c</sup> Yijing Liu,<sup>a</sup> Zhen Yang,<sup>a</sup> Fuwu Zhang,<sup>a</sup> Wenpei Fan,<sup>a</sup> Jibin Song,<sup>a</sup> Zijian Zhou,<sup>a</sup> Changyou Gao,<sup>c</sup> Feihe Huang,<sup>\*b</sup> and Xiaoyuan Chen<sup>\*a</sup>

<sup>a</sup> *Laboratory of Molecular Imaging and Nanomedicine, National Institute of Biomedical Imaging and Bioengineering, National Institutes of Health, Bethesda, Maryland 20892, United States; Email:*

[shawn.chen@nih.gov](mailto:shawn.chen@nih.gov)

<sup>b</sup> *State Key Laboratory of Chemical Engineering, Center for Chemistry of High-Performance & Novel Materials, Department of Chemistry, Zhejiang University, Hangzhou 310027, P. R. China; Email:*

[fhuang@zju.edu.cn](mailto:fhuang@zju.edu.cn)

<sup>c</sup> *MOE Key Laboratory of Macromolecular Synthesis and Functionalization, Department of Polymer Science and Engineering, Zhejiang University, Hangzhou 310027, P. R. China; Email: [zwmiao@zju.edu.cn](mailto:zwmiao@zju.edu.cn)*

# These authors contributed equally to this work

## Electronic Supplementary Information

1. *Materials and methods*
2. *Syntheses of **PyN** and **P6***
3. *Characterizations of the supramolecular hybrid material*
4. *In vitro PA imaging studies*
5. *References*

## 1. Materials and methods

1-Pyrenemethanol, 6-hydroxy-2-naphthalenesulfonic acid sodium salt, 1,10-dibromodecane, potassium carbonate and other reagents were purchased from Sigma-Aldrich and used as received. Solvents were either employed as purchased or dried according to procedures described in the literature. **P6** was synthesized according to reported method.<sup>S1</sup> <sup>1</sup>H NMR and <sup>13</sup>C NMR spectra were recorded on a Bruker Avance III-300 spectrometer or a Bruker Avance III-400 spectrometry with internal standard TMS. 2D NOESY spectrum was collected on a Bruker Avance DMX-500 spectrometer. UV-vis spectra were taken on a GENESYS 10S UV-Vis spectrophotometer. The fluorescence titration experiments were conducted on a HITACHI F-7000 spectrofluorophotometer. Mass spectra were recorded on a Micromass Quattro II triplequadrupole mass spectrometer using electrospray ionization and analyzed with the MassLynx software suite or a Bruker Esquire 3000 plus mass spectrometer (Bruker-Franzen Analytik GmbH, Bremen, Germany) equipped with an ESI interface and an ion trap analyzer. Transmission electron microscopy (TEM) studies were conducted on the FEI Tecnai12 transmission electron microscope (FEI, Hillsboro, Oregon) operating at an accelerating voltage of 120 kV. Images were acquired using a Gatan 2k X 2k cooled CCD camera (Gatan, Pleasanton, CA). Zeta potential measurements were carried out on using a SZ-100 Nanoparticle Size & Zeta Potential Analyzer. AFM imaging was conducted in air, using gentle tapping-mode AFM with a PicoForce Multimode AFM (Bruker, CA) consisting of a Nanoscope® V controller, a type E scanner head, and a sharpened TESP-SS (Bruker, CA) or similar AFM cantilever.

**Preparation of Supramolecular Hybrid.** GO@CP6⊃PyN hybrids were prepared by sonication of CP6⊃PyN (500 mg) in H<sub>2</sub>O (100 mL) with 50 mg of GO for 4 h. After the sonication, the supernatant was dialyzed against H<sub>2</sub>O to remove excess free CP6⊃PyN from the solution.

**Detection of CO<sub>2</sub> Release.** GO@CP6⊃PyN (1.00 g) was dispersed in water (20 mL). Upon NIR laser irradiation (0.5 W/cm<sup>2</sup>, 808 nm) for different time periods, the solution was lyophilized and weighted. The bicarbonate counterions were decomposed into carbonate when the solution temperature increased higher than 50 °C. Therefore the release percentage of CO<sub>2</sub> upon different irradiation time period could be calculated according to the weight changes.

**Measurement of Photothermal Effect.** The samples (CP6⊃PyN, GO and GO@CP6⊃PyN) were diluted into different concentrations with PBS, and PBS was used as a control group. A total of 200 μL of each solution was exposed upon an 808 nm NIR laser for 2 min with different laser powers. A laser energy meter (Coherent Portland, OR, USA) was used to calibrate and measure the laser densities. The temperatures changes of the solution were monitored with an IR thermal imaging system.

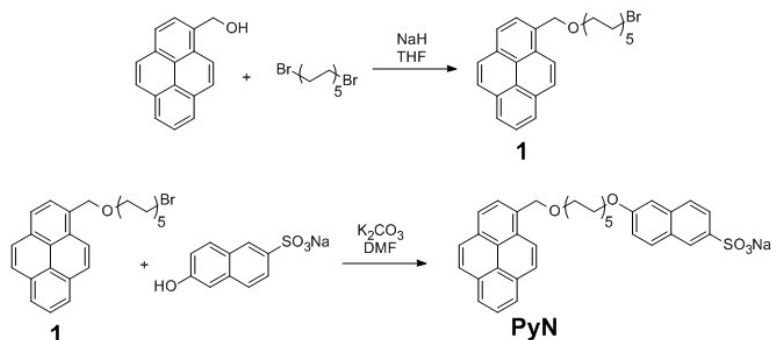
**Cell Cultures.** U87MG cell line was purchased from American Type Culture Collection (ATCC, Rockville MD). U87MG cells were cultured in Eagle's MEM (EMEM) containing 4mM L-glutamine, 4500 mg L<sup>-1</sup> glucose, 10% fetal bovine serum (FBS), 100 units per ml penicillin, and 100 units per ml streptomycin, supplied by GE Life Sciences Co. Ltd. The cell line has passed the conventional tests of cell line quality control methods (e.g., morphology, isoenzymes, and mycoplasma). Cells grew as a monolayer and were detached upon confluence using trypsin (0.5% w/v in phosphate-buffered saline). The cells were harvested from cell culture medium by incubating in the trypsin solution for 5 min. The cells were centrifuged, and the supernatant was discarded. A 3.00 mL portion of serum-supplemented medium was added to neutralize any residual trypsin. The cells were resuspended in serum-supplemented medium at a concentration of  $1.00 \times 10^4$  cells/mL. Cells were cultured at 37 °C and 5% CO<sub>2</sub>.

**Evaluation of cytotoxicity.** The cytotoxicities of GO, P6, PyN and GO@CP6⊃PyN against U87MG cell were determined by MTT assays in a 96-well plate. U87MG cells were seeded at a density of  $1 \times 10^4$  cells per well in a 96-well cell culture plate, and incubated for 24 h for attachment. Then the cells were cultured with GO, P6, PyN and GO@CP6⊃PyN at various concentrations for 12 h. After washing the cells with PBS buffer, 20 μL MTT solution (5 mg mL<sup>-1</sup>) was added to each well. The MTT solution was removed after 4 h incubation, and the cells were washed with PBS for three times. 100 μL DMSO was added to each well to solubilize formazan crystals, and the absorbance of the formazan product was measured at 570 nm using a spectrophotometer (Bio-Rad Model 680). All experiments were carried out with five replicates.

**Animal Models.** All animal experiments were performed under a National Institutes of Health Animal Care and Use Committee (NIHACUC) approved protocol. A total of  $5 \times 10^6$  human glioblastoma U87MG cells were subcutaneously injected into the right flank of 6–7 week old athymic nude mice (Harlan). The mice were used for PA imaging when the tumor reached about 500 mm<sup>3</sup>.

**Photoacoustic Imaging *in Vivo*.** A total of 20 μL of PBS, CP6⊃PyN, GO, GO@WP6⊃PyN, or GO@CP6⊃PyN solution (250 μg/mL) was intratumorally injected into the mice bearing U87MG tumor. PA imaging of tumor was performed with a Vevo 2100 LAZR system (VisualSonics, Inc., New York, NY).

## 2. Syntheses of **PyN** and **P6**



**Scheme S1.** Synthetic route to **PyN**.

Synthesis of **PyN**: **1**<sup>S2</sup> (2.25 g, 5.00 mmol) and K<sub>2</sub>CO<sub>3</sub> (8.28 g, 60.0 mmol) were added to a solution of 6-hydroxy-2-naphthalenesulfonic acid sodium salt (5.14 g, 20.0 mmol) in DMF (100 mL). The mixture was heated in a three-necked flask under nitrogen atmosphere at reflux for 24 h. The cooled reaction mixture was filtered. The filtrate was evaporated under vacuum, and the residue was further washed with water (3 × 100 mL) to afford **PyN** as a yellowish solid (2.06 g, 67%), M.p.>200 °C. The proton NMR spectrum of **PyN** is shown in Figure S1. <sup>1</sup>H NMR (300 MHz, DMF-*d*<sub>7</sub>, room temperature)  $\delta$  (ppm): 8.67 (d, *J* = 9.0 Hz, 1H), 8.51 (m, 3H), 8.40 (s, 2H), 8.03 (d, *J* = 9.0 Hz, 3H), 7.94 (d, *J* = 6.0 Hz, 3H), 7.56 (s, 2H), 7.37 (d, *J* = 9.0 Hz, 2H), 5.44 (s, 2H), 4.43 (t, *J* = 9.0 Hz, 4H), 2.08–2.00 (m, 4H), 1.67–1.49 (m, 12H). The <sup>13</sup>C NMR spectrum of **PyN** is shown in Figure S2. <sup>13</sup>C NMR (75 MHz, DMF-*d*<sub>7</sub>, room temperature)  $\delta$  (ppm): 158.55, 157.67, 157.63, 157.59, 157.53, 152.25, 134.77, 133.72, 130.09, 129.96, 128.11, 127.74, 127.55, 127.45, 127.30, 127.11, 126.49, 126.16, 125.65, 125.54, 125.18, 124.42, 123.94, 119.15, 118.43, 106.86, 70.29, 68.65, 68.03, 33.23, 33.14, 30.94, 28.99, 27.63, 26.89, 26.76, 26.33. LRESIMS is shown in Figure S3: *m/z* 593.2 [M – Na]<sup>–</sup> (100%). HRESIMS: *m/z* calcd for [M – Na]<sup>–</sup> C<sub>37</sub>H<sub>37</sub>O<sub>5</sub>S, 593.2367, found 593.2375, error 1.3 ppm.

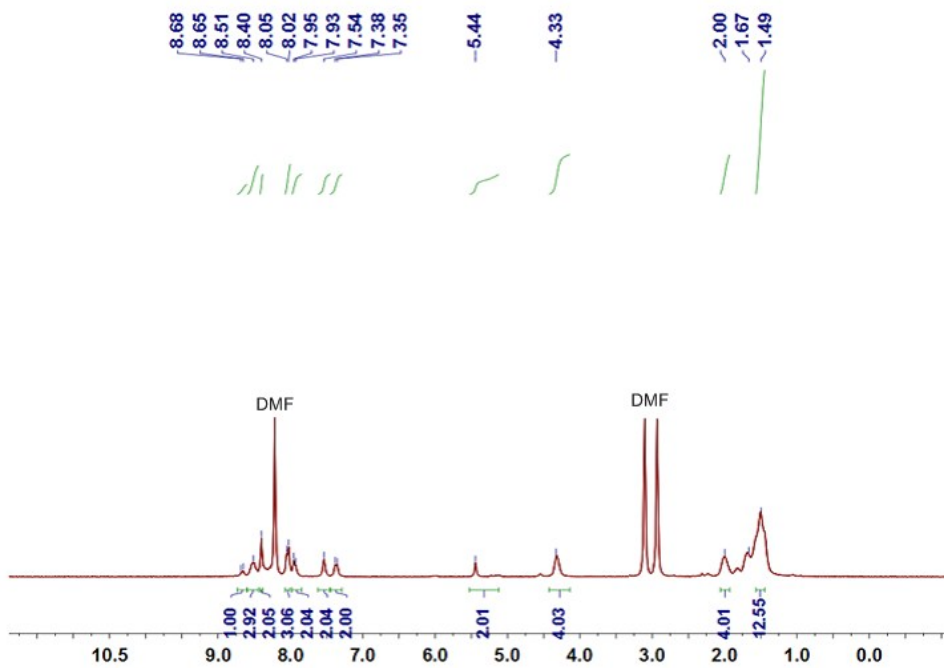


**Figure S1.**  $^1\text{H}$  NMR spectrum (300 MHz,  $\text{DMF-}d_7$ , room temperature) of **PyN**.

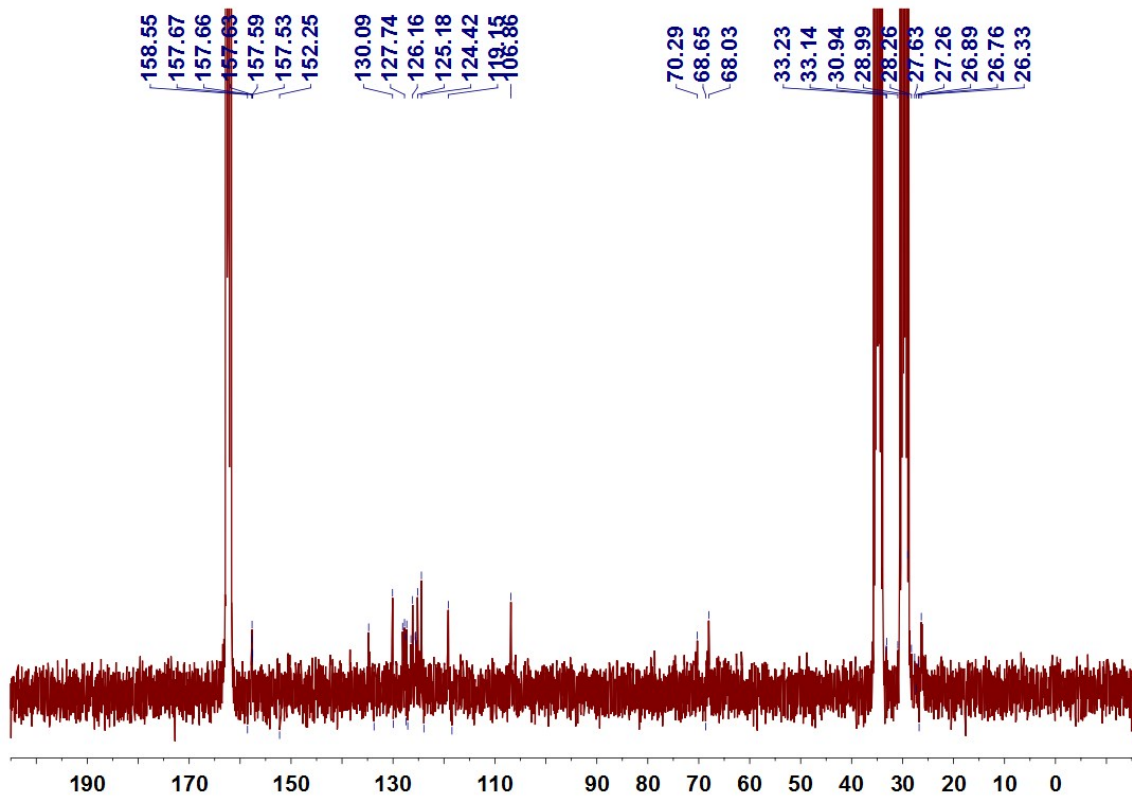


**Figure S2.**  $^{13}\text{C}$  NMR spectrum (75 MHz,  $\text{DMF-}d_7$ , room temperature) of **PyN**.

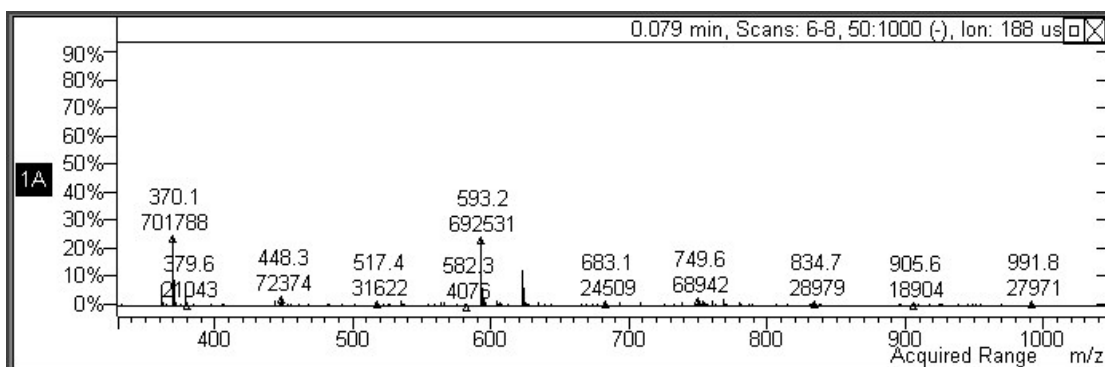
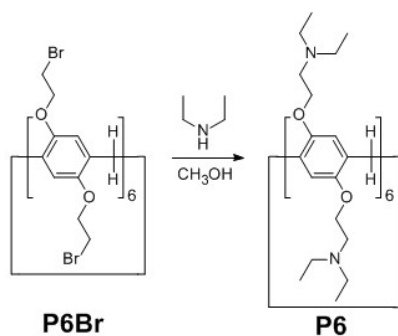


**Figure S3.** Electrospray ionization mass spectrum of **PyN**. Assignment of the main peak:  $m/z$  593.2 [ $M - Na$ ]<sup>-</sup> (100%).



**Scheme S2.** Synthetic route to **P6**.

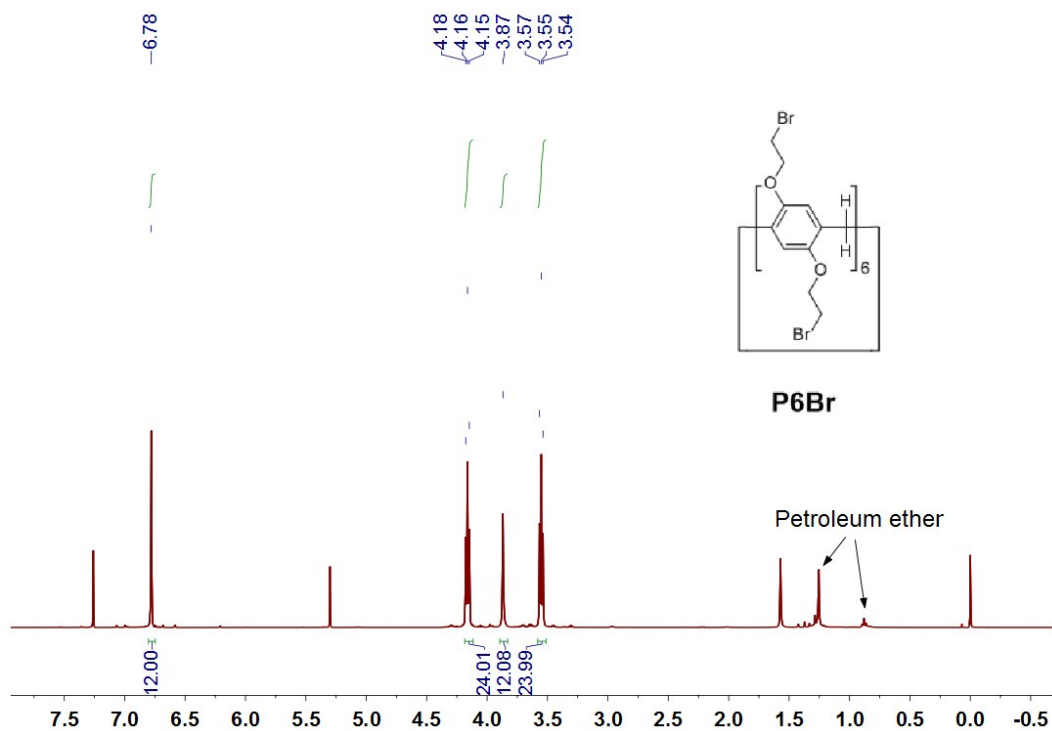


**Figure S4.** <sup>1</sup>H NMR spectrum (400 MHz, chloroform-*d*, room temperature) of **P6Br**.

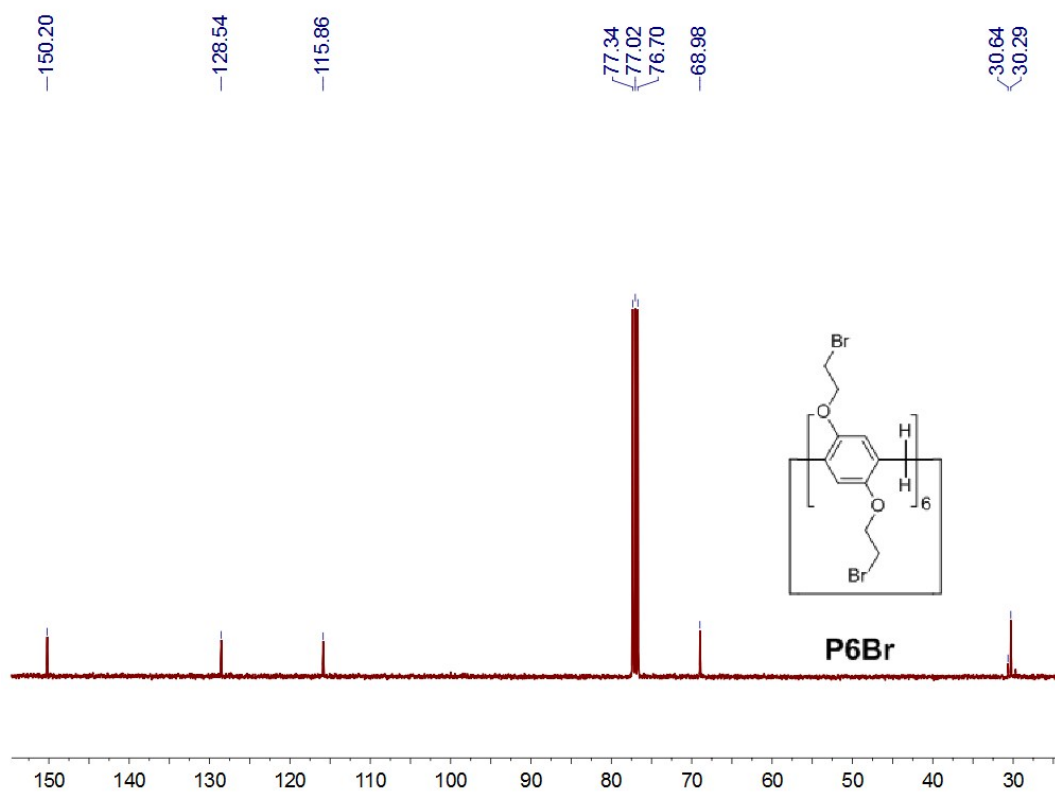


**Figure S5.**  $^{13}\text{C}$  NMR spectrum (100 MHz, chloroform-*d*, room temperature) of **P6Br**.

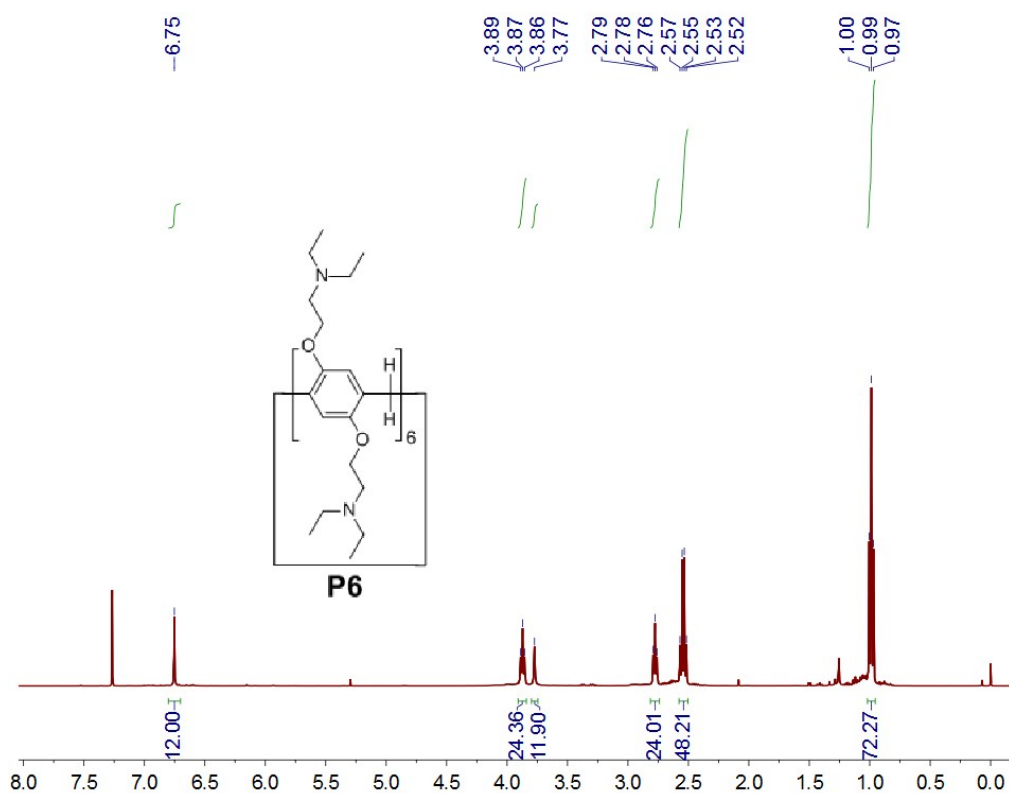


**Figure S6.**  $^1\text{H}$  NMR spectrum (400 MHz, chloroform-*d*, room temperature) of **P6**.

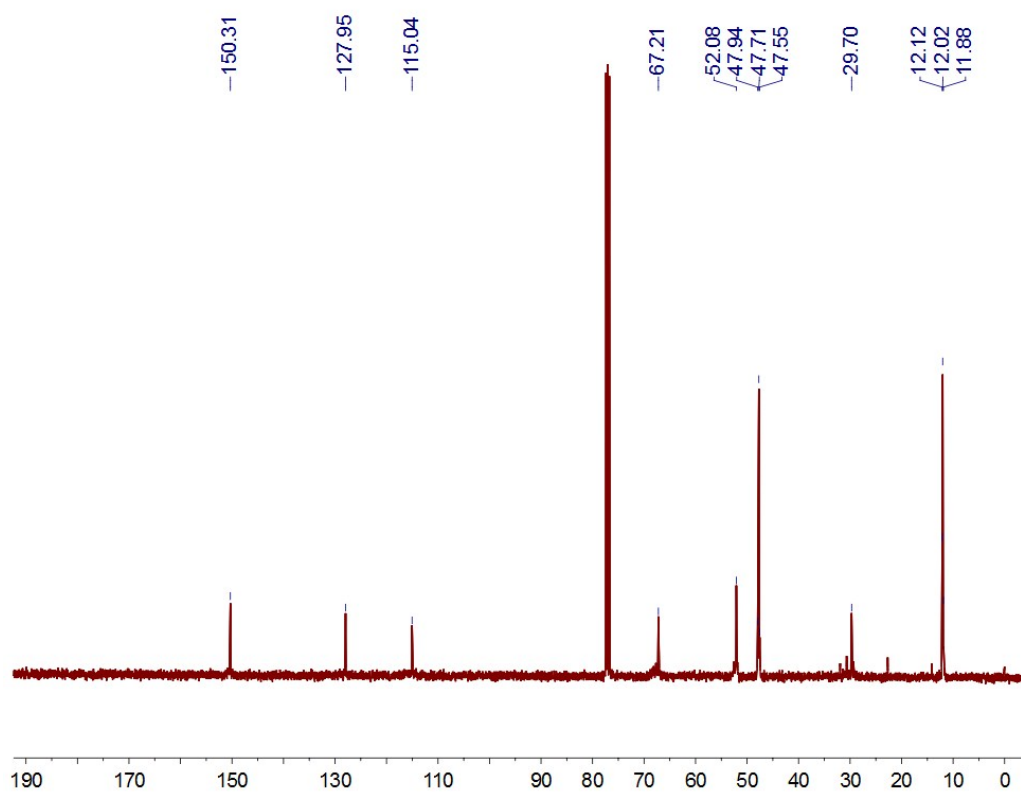


**Figure S7.**  $^{13}\text{C}$  NMR spectrum (100 MHz, chloroform- $d$ , room temperature) of **P6**.

### 3. Characterizations of the supramolecular hybrid material

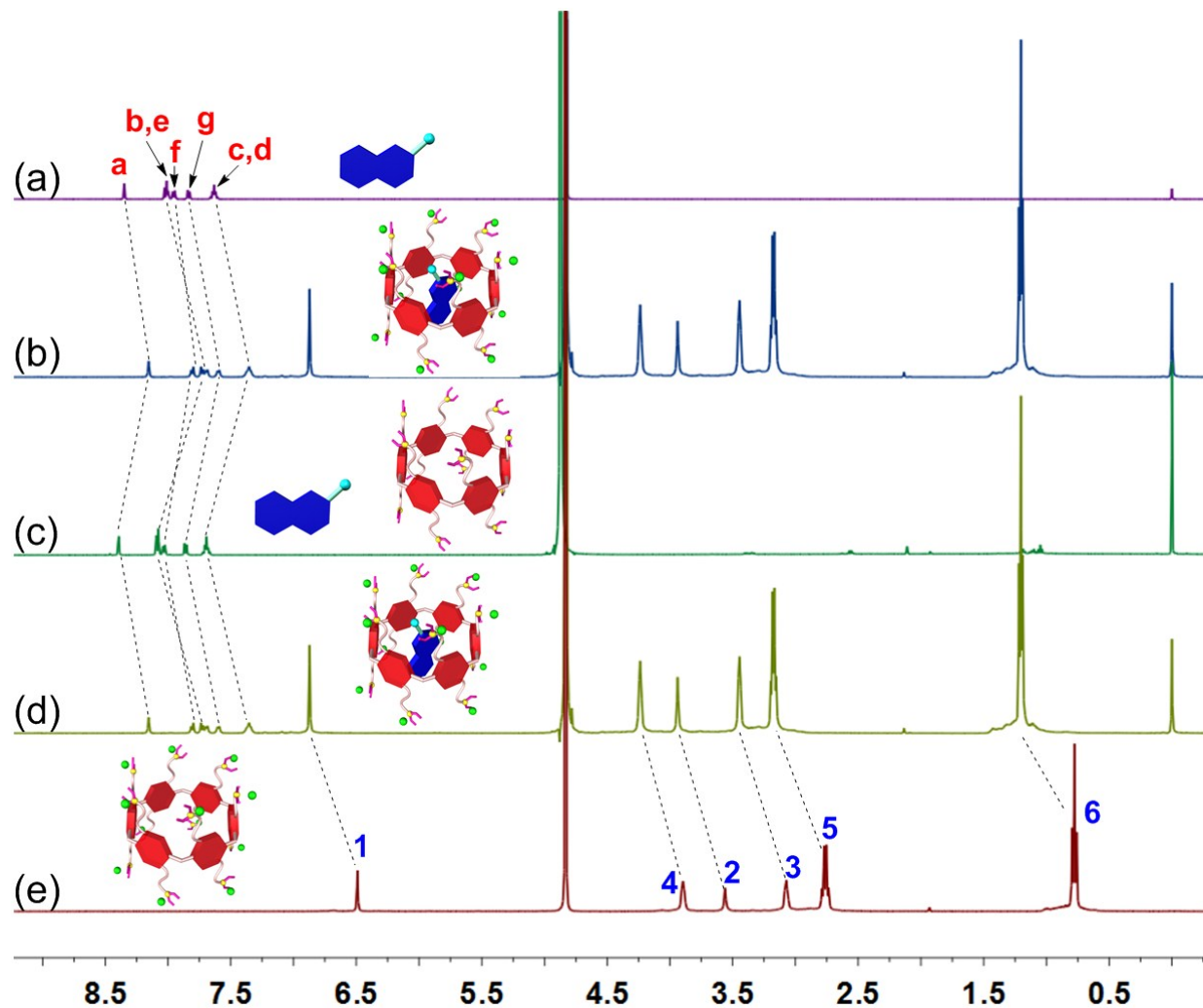


**Figure S8.** Partial <sup>1</sup>H NMR (400 MHz, D<sub>2</sub>O, room temperature) of (a) **M** (2.00 mM), (b) **M** (2.00 mM) and **CP6** (2.00 mM), (c) **M** (2.00 mM) and **CP6** (2.00 mM) after bubbling N<sub>2</sub> for 5 min, (d) **M** (2.00 mM) and **CP6** (2.00 mM) after bubbling N<sub>2</sub> for 5 min and then CO<sub>2</sub> for 5 min, and (e) **CP6** (2.00 mM).

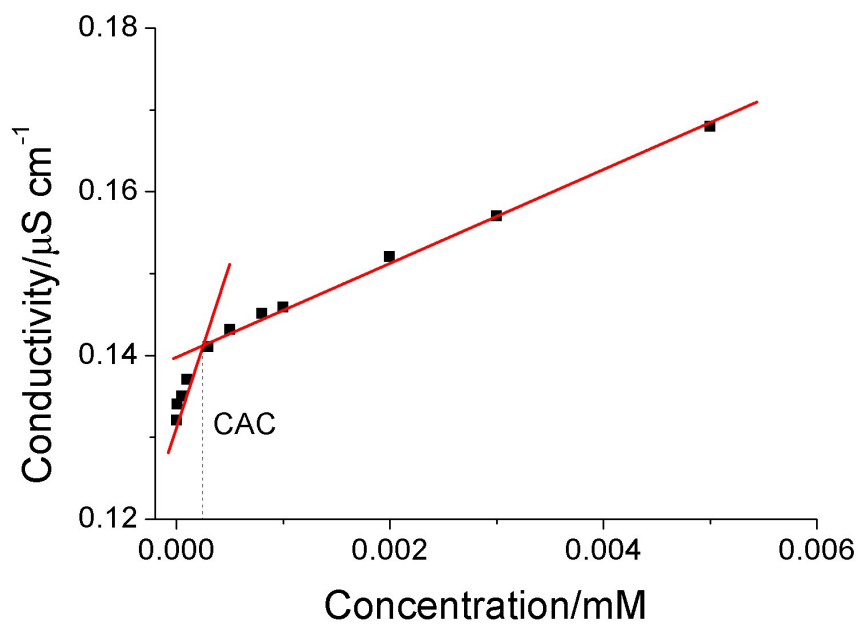


**Figure S9.** The concentration-dependent conductivity of PyN. The critical aggregation concentration was determined to be  $2.43 \times 10^{-7}$  M.

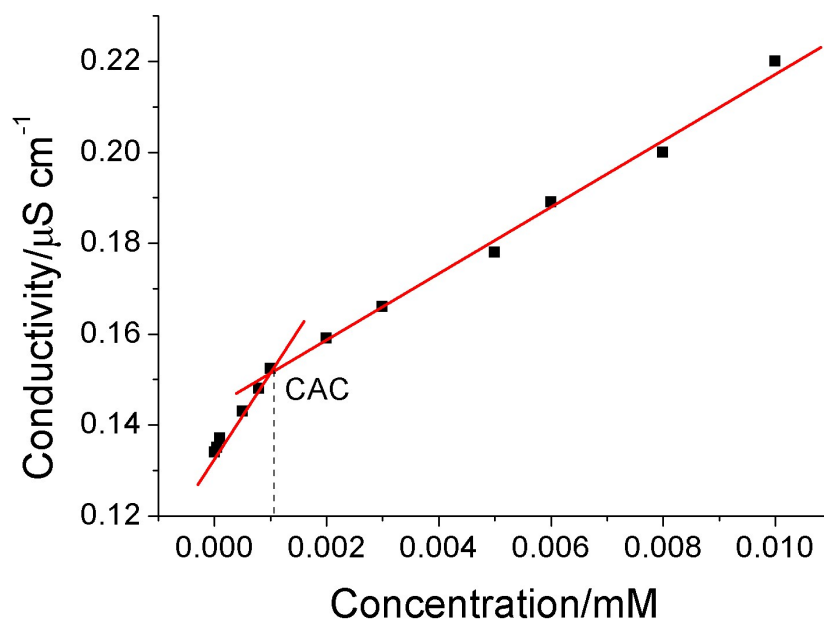


**Figure S10.** The concentration-dependent conductivity of CP6 $\supset$ PyN. The critical aggregation concentration was determined to be  $1.07 \times 10^{-6}$  M.

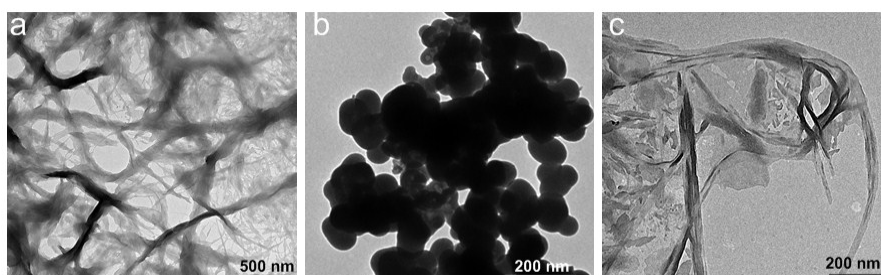


**Figure S11.** TEM image of (a) PyN, (b) CP6 $\supset$ PyN, and (c) CP6 $\supset$ PyN after bubbling N<sub>2</sub> for 5 min.

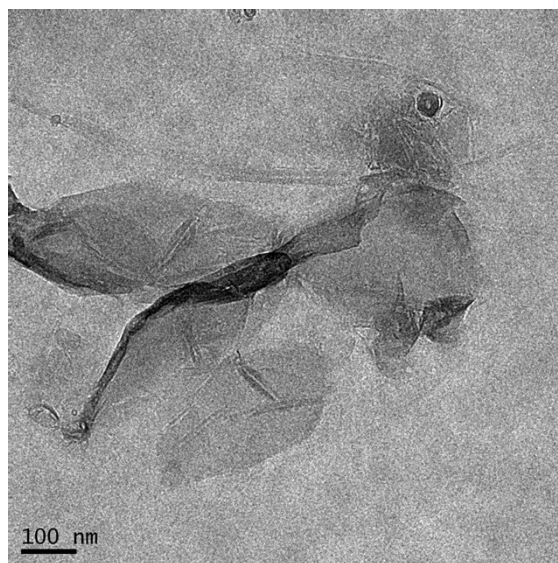


**Figure S12.** TEM image of GO@CP6 $\supset$ PyN.

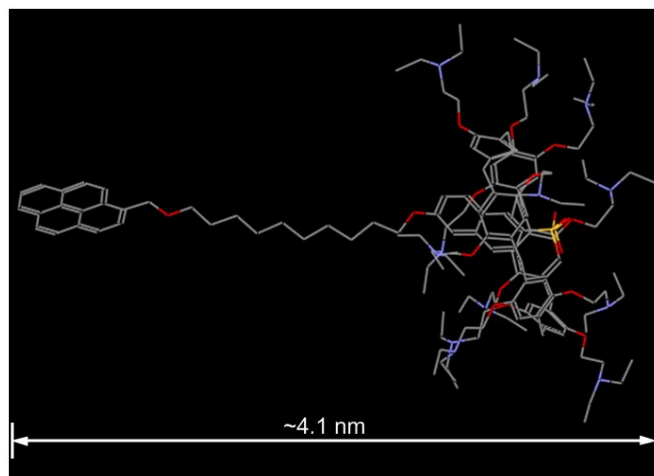


**Figure S13.** The energy-minimized structure of the host-guest complex obtained from Chem 3D. All hydrogens and counterions were omitted for clarity.

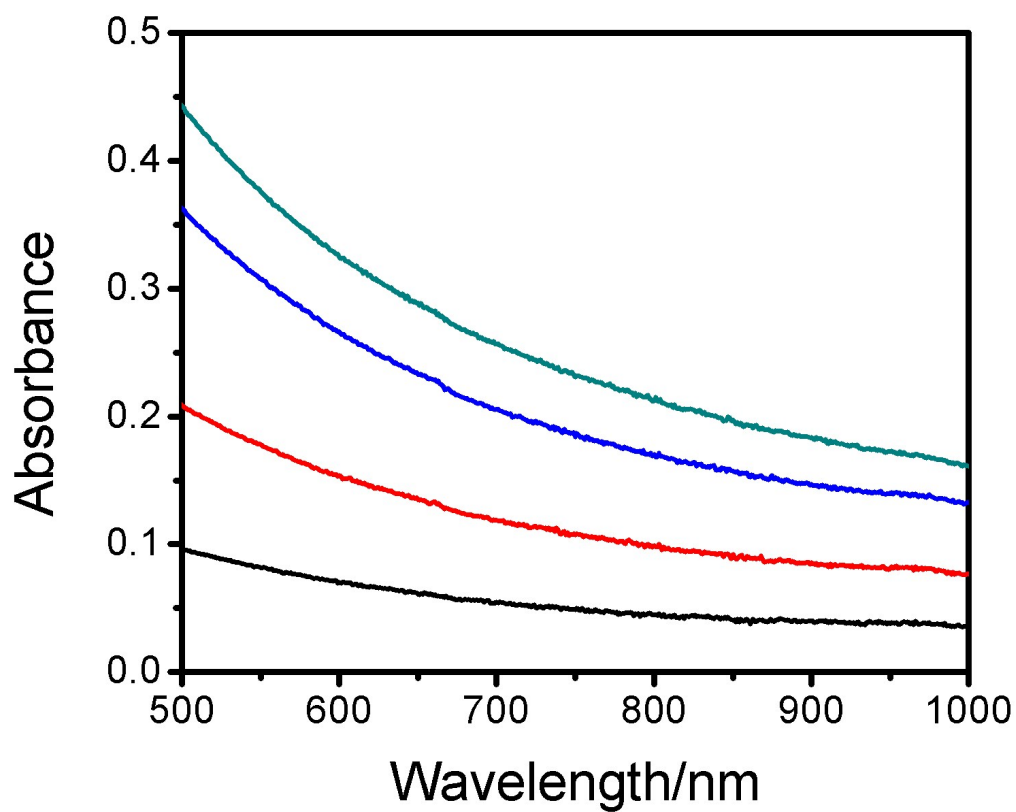


*Figure S14.* UV-vis spectra of GO upon gradual addition of CP6-PyN.

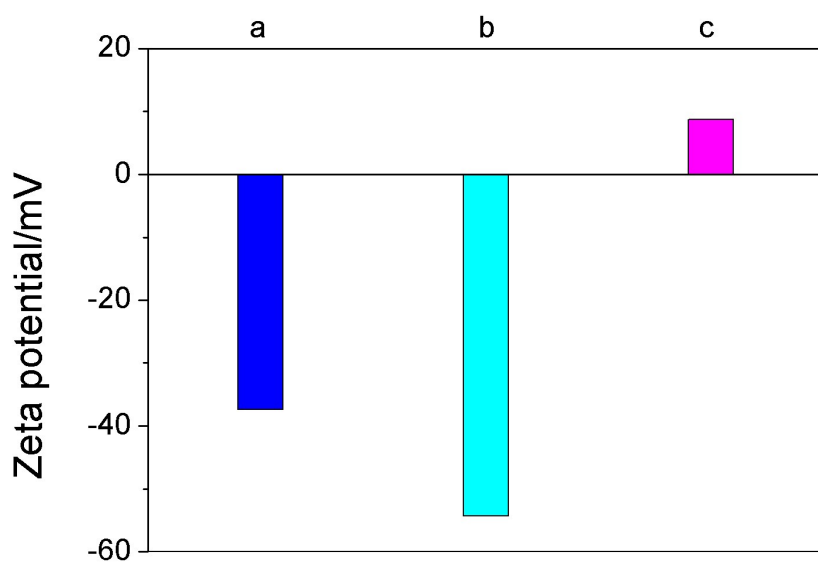


*Figure S15.* Zeta potential of (a) GO, (b)GO@PyN, and (c) GO@CP6-PyN.

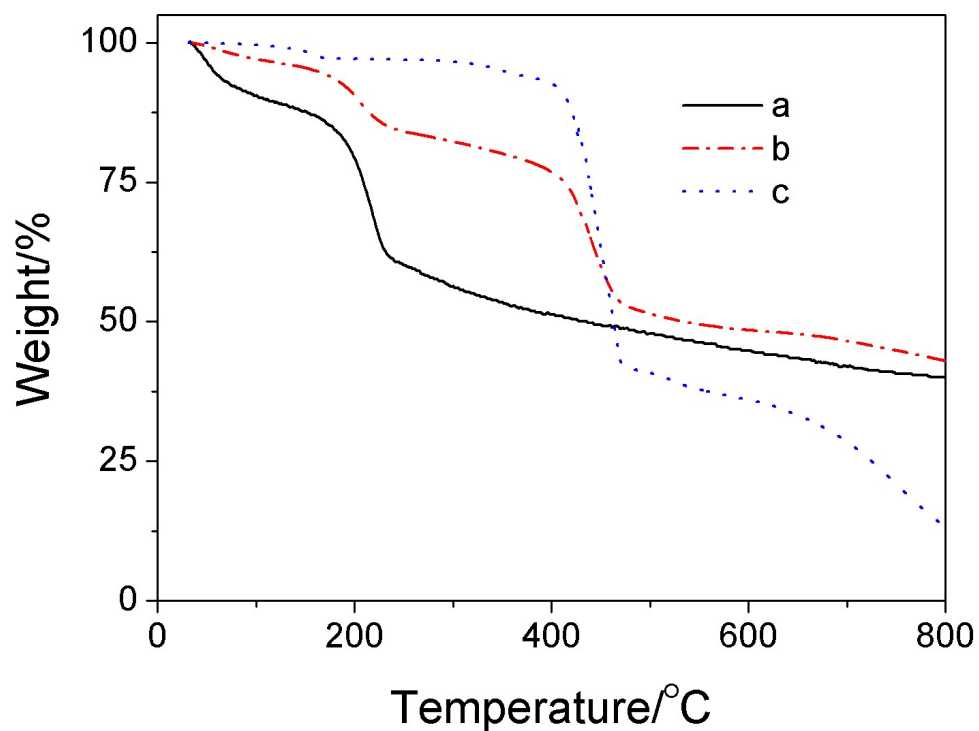


**Figure S16.** TGA curves of (a) GO, (b) GO@CP6⊃PyN, and (c) CP6⊃PyN.

#### 4. *In vitro* PA imaging studies

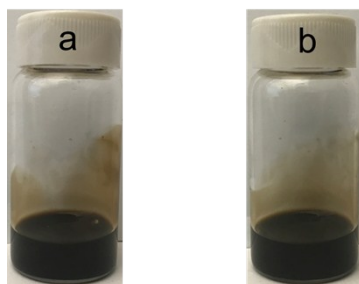


**Figure S17.** (a) Photograph of the aqueous solution containing GO@CP6⊃PyN. (b) Photograph of the aqueous solution containing GO@CP6⊃PyN after standing for 2 months.

The supramolecular hybrid GO@CP6⊃PyN was quite stable. As shown in Fig. S17, no precipitation was observed for the aqueous solution containing GO@CP6⊃PyN after standing for 2 months.

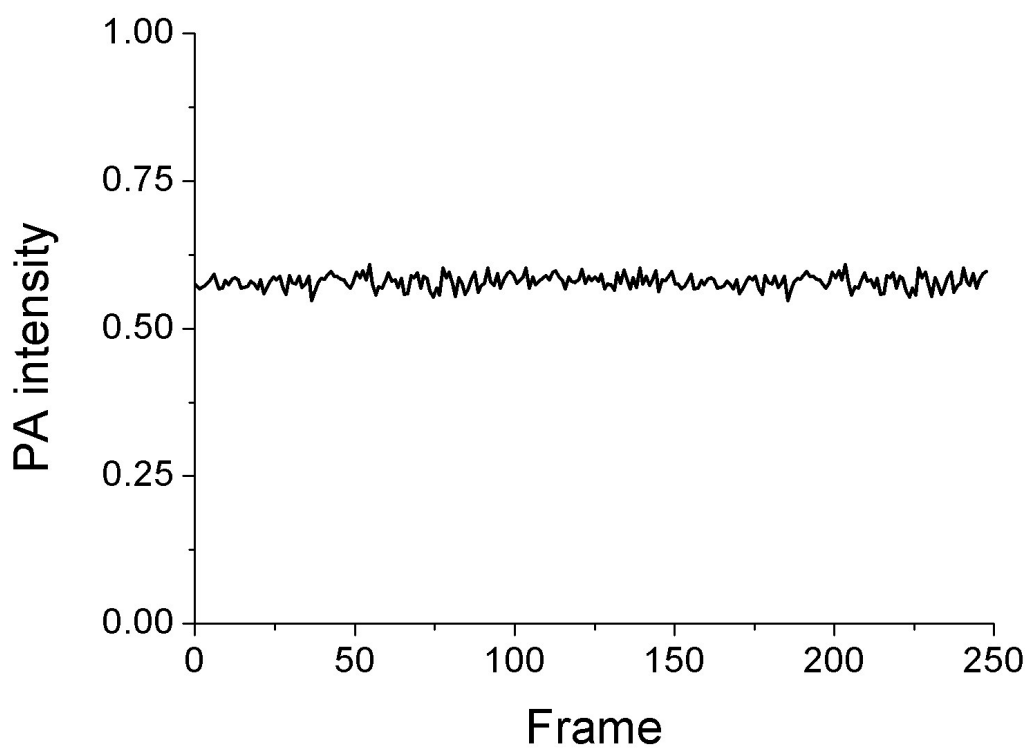


*Figure S18.* PA intensity changes of PBS at 808 nm over time.

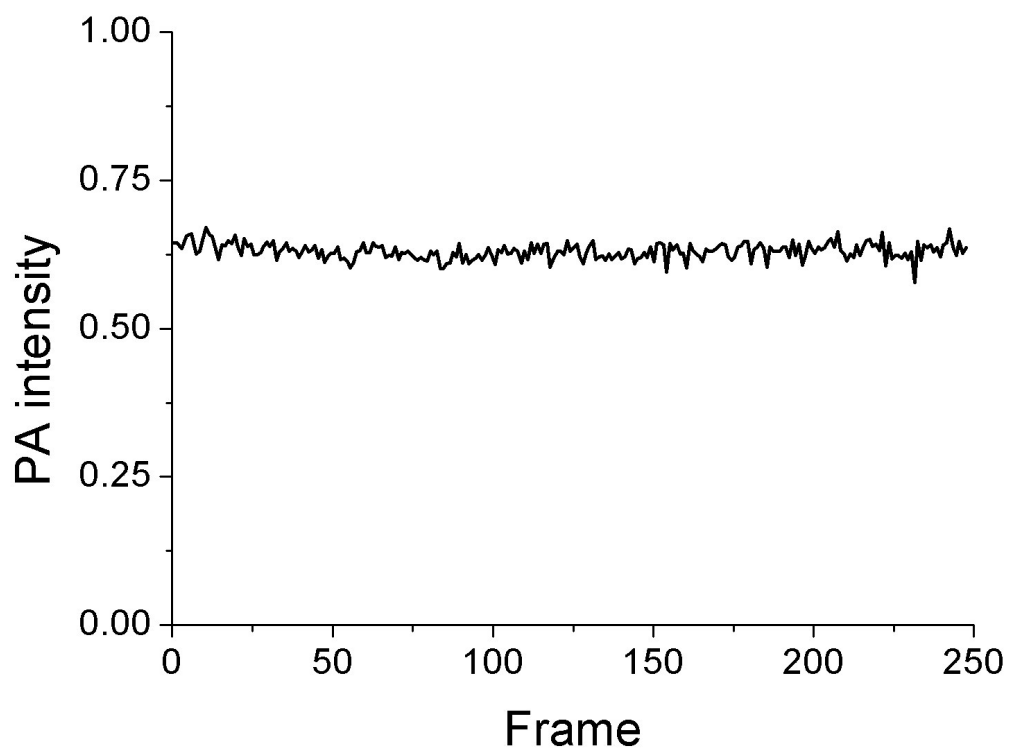


*Figure S19.* PA intensity changes of CP6 to PyN at 808 nm over time.

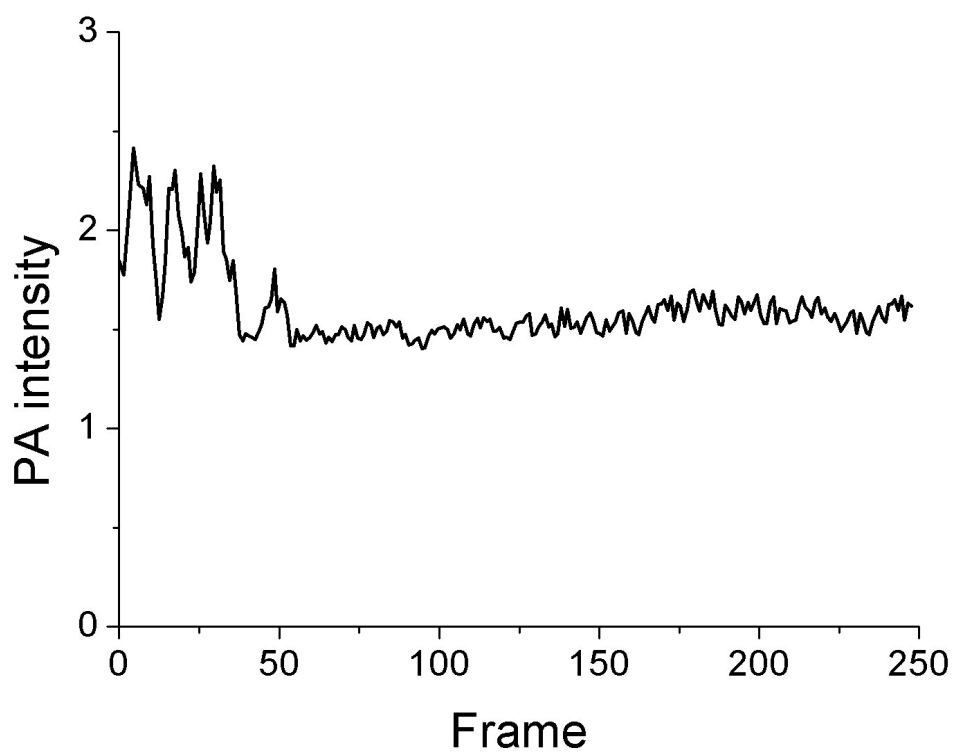


*Figure S20.* PA intensity changes of GO at 808 nm over time.

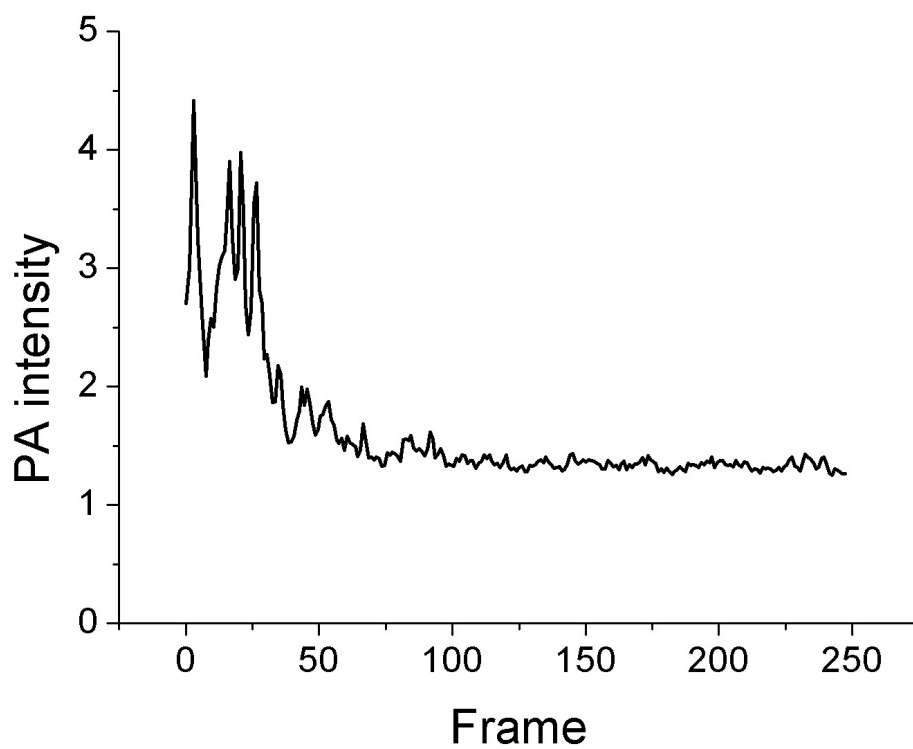


*Figure S21.* PA intensity changes of GO@WP6@PyN at 808 nm over time.

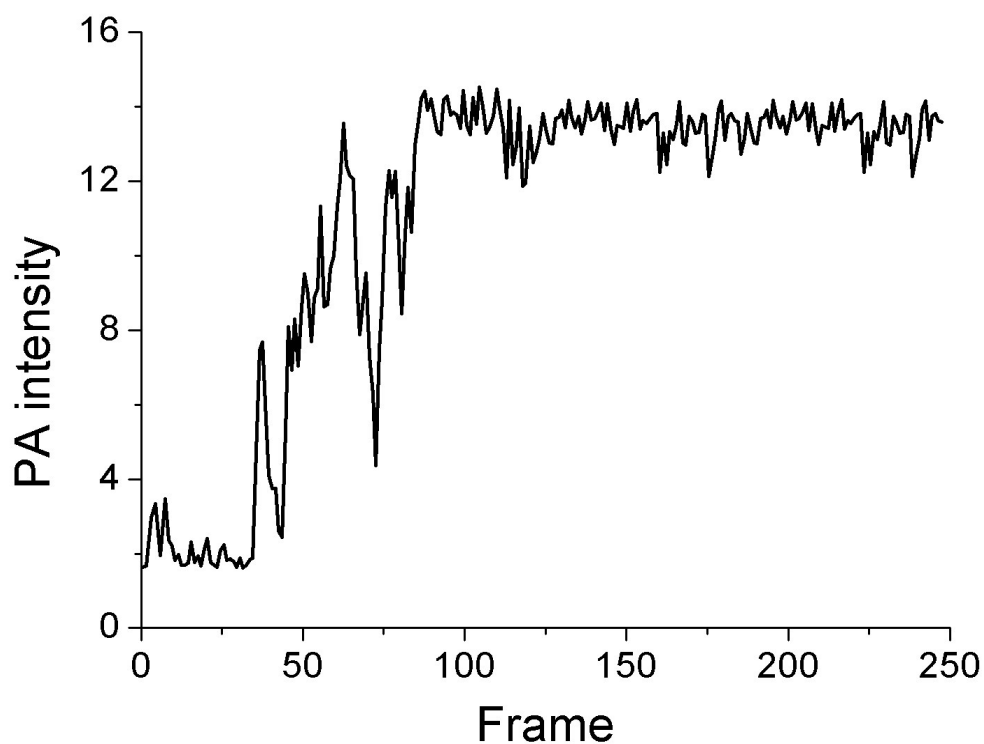


**Figure S22.** PA intensity changes of GO@CP6⊃PyN at 808 nm over time.

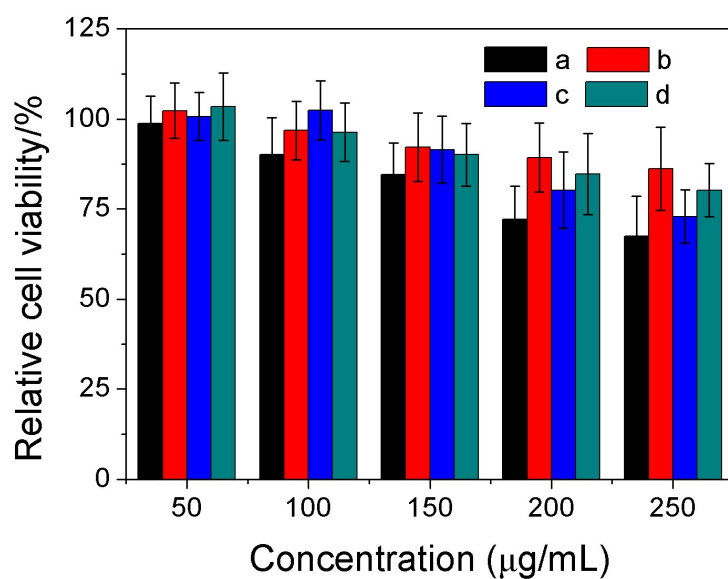


**Figure S23.** MTT assay of (a) P6, (b) PyN, (c) GO and (d) GO@CP6⊃PyN against U87MG cells.

As shown in Fig. S23, the relative cell viability was higher than 80% for GO@CP6⊃PyN even at a high concentration (250 µg/mL), confirming the excellent biocompatibility of this supramolecular hybrid material.

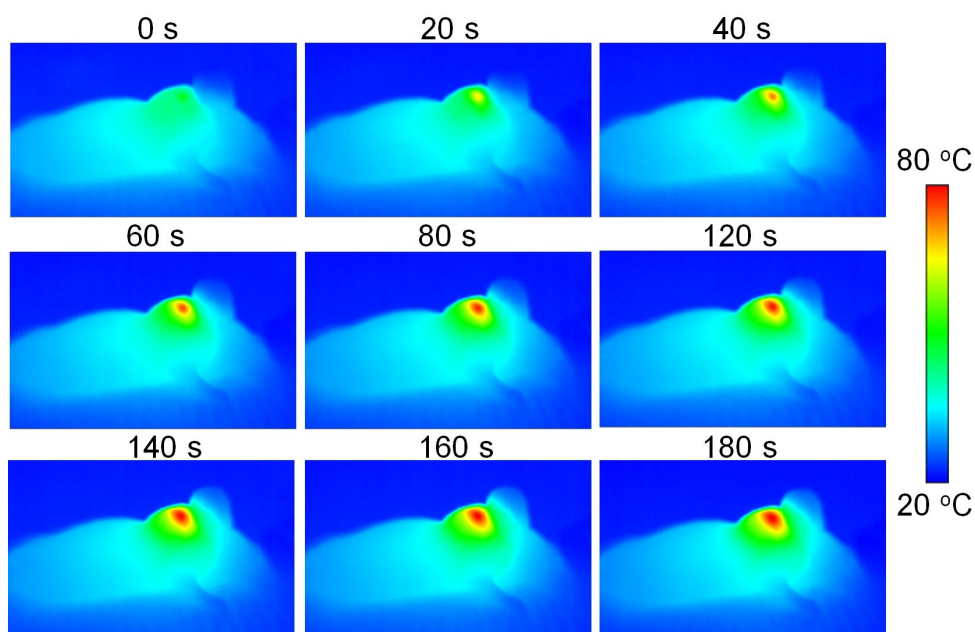


**Figure S24.** Representative thermal images of U87MG tumor-bearing mice (tumor sites) subjected to laser irradiation (808 nm, 1.0 W/cm<sup>2</sup>) for 3 min after injection of GO@CP6 $\supset$ PyN.

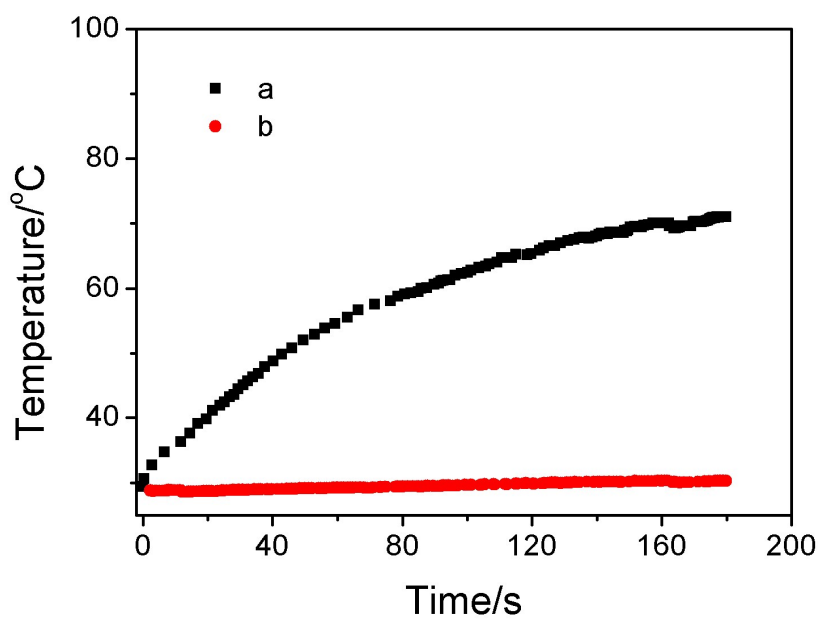


**Figure S25.** Temperature change curves determined by thermographic camera after treatments of the mice bearing U87MG tumors with (a) GO@CP6 $\supset$ PyN or (b) PBS upon exposure to the 808 nm laser at a power density of 1.0 W/cm<sup>2</sup>.

### References

- S1 K. Jie, Y. Zhou, Y. Yao, B. Shi, F. Huang, *J. Am. Chem. Soc.* **2015**, *137*, 10472–10475.  
 S2 M. Hariharan, J. Joseph, D. Ramaiah, *J. Phys. Chem. B* **2006**, *110*, 24678–24686.